Journal of Innovative Optical Health Sciences
Vol. 4, No. 2 (2011) 151−158

DOI: 10.1142/S1793545811001332

PHASE DIFFERENCE BETWEEN LOW-FREQUENCY OSCILLATIONS OF CEREBRAL DEOXY- AND OXY-HEMOGLOBIN CONCENTRATIONS DURING A MENTAL TASK

ANGELO SASSAROLI, FENG ZHENG, MICHELE PIERRO,
PETER R. BERGETHON and SERGIO FANTINI*
Department of Biomedical Engineering, Tufts University
4 Colby Street, Medford, MA 02155, USA
**sergio.fantini@tufts.edu*

Hemodynamic low-frequency (∼0.1 Hz) spontaneous oscillations as detected in the brain by near-infrared spectroscopy have potential applications in the study of brain activation, cerebral autoregulation, and functional connectivity. In this work, we have investigated the phase lag between oscillations of cerebral deoxy- and oxy-hemoglobin concentrations in the frequency range 0.05−0.10 Hz in a human subject during a mental workload task. We have obtained a measure of such phase lag using two different methods: (1) phase synchronization analysis as used in the theory of chaotic oscillators and (2) a novel cross-correlation phasor approach. The two methods yielded comparable initial results of a larger phase lag between low-frequency oscillations of deoxy- and oxy-hemoglobin concentrations during mental workload with respect to a control, rest condition.

Keywords: Phase lag; oxyhemoglobin; deoxyhemoglobin; phase synchronization; cross-correlation phasor; LFO.

1. Introduction

Near-infrared spectroscopy (NIRS) has been widely used to investigate hemodynamic signatures of brain activation under a variety of stimulation protocols.[1−4] In the last decade, the discovery by functional magnetic resonance imaging (fMRI) studies that the brain can be shown to have apparent functional connectivity by monitoring hemodynamic patterns, especially in the resting state or default-mode, has led to much interest in understanding the relationship of these default-mode networks. The default-mode networks appear to be active during self-reflection and are suppressed during tasks involving salient external stimuli.[5,6] Given the sensitivity of NIRS signals to hemodynamic changes in the brain parenchyma, there has been an interest in expanding the use of NIRS toward investigations into these resting state and salience networks, especially including studies of spontaneous low-frequency oscillations (LFOs) at frequencies in the order of 0.1 Hz. Examples of such studies include a differentiation between normal and pathological processes involving autoregulation[7] and assessment of functional connectivity networks.[8−10] Although the average penetration depth of light in the NIRS wavelength range limits its applicability to the cerebral cortex, its features, such as the sensitivity to both oxy- and deoxy-hemoglobin species, portability, and continuous monitoring capability, render NIRS a suitable technique for studying human subjects in everyday environments and in cases that allow more natural mobility. In the field of functional connectivity, one typically studies temporal correlations between remote areas of the brain. The few NIRS studies

that have appeared in the literature on this topic have used the Pearson coefficient to quantify the temporal correlation between tissue concentrations of hemoglobin species in different regions of the brain cortex.[8] Usually, one NIRS channel, corresponding to a specific brain location, is used as a "seed channel," and a correlation map is obtained by calculating the Pearson coefficient of each channel with respect to the seed channel. This approach has been widely used also in connectivity studies based on fMRI, which, however, features a lower temporal resolution ($\approx$1 s) than NIRS ($\approx$10 ms) and therefore has a reduced sensitivity to faster hemodynamic oscillations.

In this work, we explore the potential of NIRS measurements to studies of default-mode and other cognitive connectivity networks by assessing the phase relationship between deoxy- and oxy-hemoglobin cerebral concentrations based of its capacity for high temporal resolution and sensitivity to both oxygenated and deoxygenated hemoglobin species. Not only can the dynamics of phase lag between hemoglobin species find a natural application in aforementioned functional connectivity studies, it also has the potential to advance our understanding of the dynamic interplay of fundamental physiological processes, such as cerebral metabolic rate of oxygen, blood flow, and blood volume, especially if correlated with a functional network analysis of the concurrent electrophysiological activity. For example, several studies in the literature have reported out-of-phase oscillations between oxy- and deoxy-hemoglobin (i.e., phase lags different from 0 or π).[3,7,11] In a recent work, we have provided an interpretation of such results, and we have also introduced a phasor method to quantify and represent the phase relationships between hemoglobin concentration oscillations.[12] Here, we apply our phasor method to study the phase relationship between deoxy- and oxy-hemoglobin cerebral concentrations during two mental workload tasks that largely involve the working memory. The results obtained with our phasor method are similar to those obtained with the phase synchronization approach used in the dynamic characterization of chaotic oscillators,[13] and show a significant increase in the phase lag of deoxy-hemoglobin versus oxy-hemoglobin concentrations induced by the mental workload task. Based on our previous work,[12] we argue that this result is due to a re-adjustment of baseline out-of-phase spatiotemporal physiological processes during the mental task periods.

2. Experimental Setup and Activation Protocol

The NIRS instrument is a commercial multi-channel frequency-domain tissue spectrometer (OxiplexTS, ISS, Inc., Champaign, IL). This instrument features two detectors channels (Channel A and Channel B) and 16 intensity modulated laser diodes of which, in this study, we used only four, two emitting at 690 nm and two emitting at 830 nm. These four laser diodes are electronically multiplexed to time share the two optical detectors. The illumination fibers are placed on the subject's forehead according to the arrangement shown in Fig. 1. Each illumination−collection fiber pair consists of

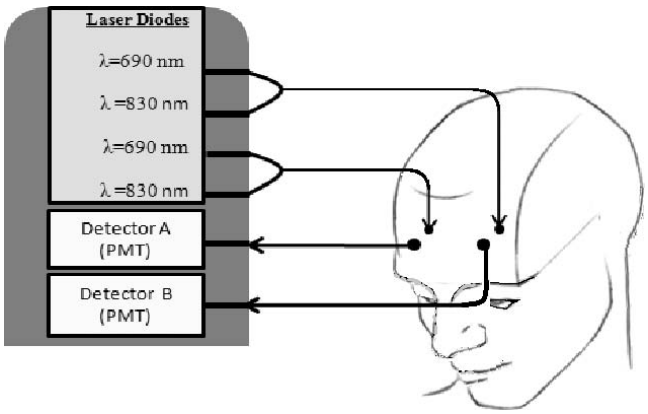

Fig. 1. Experimental setup showing the two optical probes placed on the subject's forehead, consisting of two optical detectors (Channel A: right side; Channel B: left side) and four laser diodes (two emitting at 690 nm and two at 830 nm). PMT: photomultiplier tube.

two source optical fibers (one delivering light at 690 nm and the other at 830 nm) and one detector optical fiber (A for the right side of the forehead, and B for the left side). In order to achieve sensitivity to the brain cortex, the source−detector distance on the subject's forehead is set at 3 cm. The source and detector optical fibers are held on the subject's forehead by means of a black flexible band properly arranged to support the optical probes and guarantee stable positioning of the optical probes. The acquisition time for the four source−detector pairs, as determined by the source multiplexing, is set at 6.25 Hz, so that we collect one data point every 160 ms.

A 23-year-old healthy male subject is presented with a rotating cube displayed on a computer screen. Each side of the rotating cube is made of four square sections having either the same color (case identified as workload 0) or one of four different colors (case identified as workload 4). Workload 0 is considered a low-working memory demand condition compared to workload 4. During workload 4, the subject is asked to keep track of the number of square sections of each color. Every side is shown to the subject for 8 s; after that, the cube undergoes a 90° rotation (for 3 s) showing a new side of the cube to the subject. The total time for a complete rotation is 45 s and is followed by a rest period of 40 s for a total workload-rest period of 85 s. During the rest period, no cube is displayed on the screen and the subject is instructed to avoid any mental task. The whole experiment includes six workload 0 and six workload 4 epochs, randomly mixed and all separated by a rest epoch. The rest epoch would represent the type of brain state found in the eyes-open "default-mode," while each of the workload states represents different cognitive loads. There is growing evidence from fMRI studies that the resting state of eyes-open with no fixation (our resting condition) is different from a low cognitive load state with fixation and attention (our workload 0 state).[14] More details on this protocol can be found in work by Sassaroli *et al.*[15]

3. Data Analysis

Optical intensity changes are translated into tissue absorption changes by means of the modified Beer−Lambert law. Differential pathlength factors of 6.5 and 5.8 are assumed at the wavelengths of 690 and 830 nm, respectively. The absorption temporal traces are processed by third-order polynomial detrending and by a band-pass elliptical filter over the frequency band 0.05−0.10 Hz. The absorption traces at the two wavelengths (690 and 830 nm) are then translated into temporal traces of oxy-hemoglobin (Δ[HbO]) and deoxy-hemoglobin (Δ[Hb]) concentrations by using the known molar extinction spectra of oxy- and deoxy-hemoglobin.

We used two methods to measure the phase lag between deoxy- and oxy-hemoglobin concentration oscillations in the selected frequency band of 0.05−0.10 Hz.

3.1. *Phase synchronization*

The concept of phase synchronization between chaotic oscillators has been described in the literature of dynamical systems and has already found applications in brain studies.[13] Briefly, a temporal signal is filtered in a relatively narrow frequency range, and a phase value is associated to each time point by using the concept of analytic continuation of a signal. The real part of the analytic continuation is the filtered signal and the imaginary part is the Hilbert transform of the filtered signal. The polar representation of the analytic continuation at each time point defines a unique amplitude and phase of the signal. If $s_1(t)$ and $s_2(t)$ are two signals, then a phase synchronization regime between them is established if one can find two integers n and m such that $|n\phi_{s1} - m\phi_{s2}| < C$, where ϕ_{si} is the phase associated with signal $s_i(t)$ and C is a fixed constant. In this study, we hypothesize a linear relationship between deoxy- and oxy-hemoglobin concentrations and we choose $n = m = 1$. The resulting condition $|\phi_{s1} - \phi_{s2}| < C$ is usually fulfilled only in a statistical sense; the phase synchronization can be temporarily lost with resulting jumps in the phase difference. Therefore, the phase relationship between two signals is appropriately described by reporting a histogram of the phase distribution. A peaked distribution is indicative of significant phase synchronization between two signals; on the contrary, a flat distribution shows no synchronization. More quantitatively, the concept of phase synchronization between two signals is defined by the Shannon entropy:

$$S = -\sum_{i=1}^{N} P_i \ln(P_i), \tag{1}$$

where i enumerates the bins in which the $0 - 2\pi$ phase range is divided, N is the number of phase bins,

and P_i is the fraction of measured phase values within bin i. The phase synchronization is quantified by defining a phase synchronization index (PSI):

$$\mathrm{PSI} = 1 - \frac{S}{\ln(N)}. \tag{2}$$

For a flat phase distribution (where $P_i = 1/N$ for all values of i), the PSI value is 0, whereas for a highly peaked distribution where all measured phase values fall within one single bin j (so that $P_i = 0$ for $i \neq j$, $P_j = 1$) the PSI value is 1. Statistical properties (e.g., average, standard deviation) and statistical tests on distributions of phase lags were based on circular statistics.[16]

3.2. *Cross-correlation phasors*

We have recently proposed an alternative method to monitor phase lags between signals over a relatively narrow frequency band using the concept of phasors.[12] Phasors are polar two-dimensional vectors characterized by amplitude (A) and phase (θ) and represent harmonic oscillations at a fixed angular frequency (ω). They are used in areas such an optics, electronics to describe monochromatic oscillations and especially to graphically compute a linear superposition of out-of-phase oscillations. In NIRS measurements of cerebral hemodynamics, one can investigate oscillations at a specific frequency by processing the data with a relatively narrow band-pass filter. We define the relative phase of two signals at a given angular frequency ω, say $x_1(t)$ and $x_2(t)$, in terms of the delay time $\tau_{\max}$ at which the absolute value of the cross-correlation function of the two signals ($|R_{x1,x2}(\tau)|$) is maximized. In an equation, the relative phase of $x_1(t)$ and $x_2(t)$ is given by $\theta_{x1,x2} = \omega\tau_{\max}$ ($+\pi$ if $R_{x1,x2}(\tau_{\max}) < 0$). We define the phasor amplitude as one-half the peak-to-peak range of the measured oscillations.

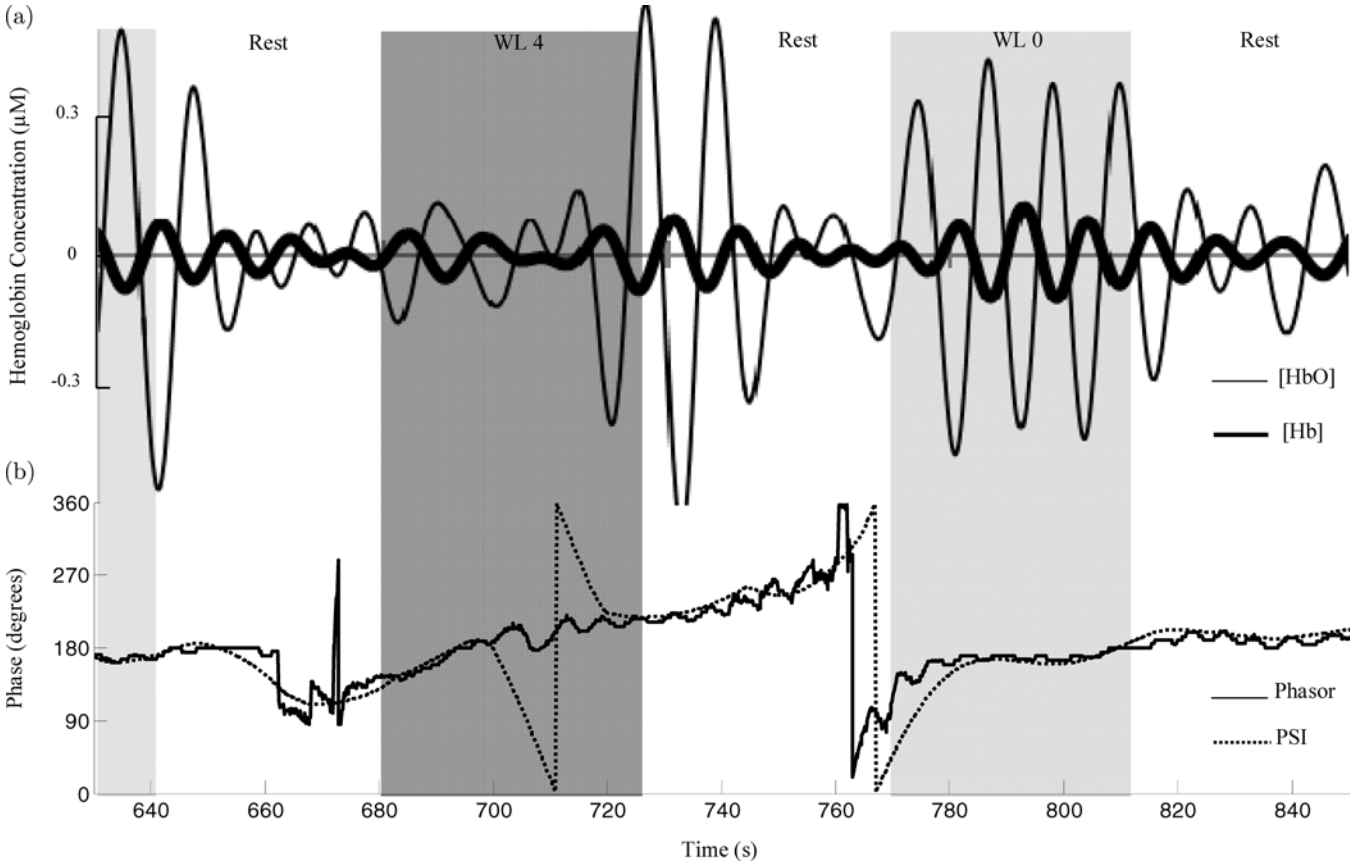

Fig. 2. (a) Band-pass filtered time traces of deoxy-hemoglobin ([Hb]) and oxy-hemoglobin ([HbO]) cerebral concentrations changes measured during a portion of the protocol including one workload 0 epoch (light shaded area labeled WL 0) and one workload 4 epoch (dark shaded area labeled WL 4). (b) Phase difference between [Hb] and [HbO] as measured with PSI and cross-correlation phasor methods.

Since the filtering process applied to the raw intensity data includes a finite range of frequencies (0.05−0.1 Hz), phase lags between hemoglobin species can originate from frequency shifts between them. In order to limit this effect in both phase synchronization and phasor methods, we used a moving window of 20 s, and we assigned the calculated phase lag to the central point. We have recorded only phase lags of [Hb] and [HbO] oscillations associated with PSI and maximum cross-correlation values that are greater than threshold values of 0.3 for the PSI and 0.75 for the cross-correlation.

4. Results

Figure 2(a) shows LFOs of deoxy- and oxy-hemoglobin concentrations (Δ[Hb] and Δ[HbO], respectively) during a section of the experimental protocol including one workload 4, one workload 0, and the associated rest periods. Figure 2(b) shows the corresponding phase lags between [Hb] and [HbO] ($\phi_{\Delta[\mathrm{Hb}]} - \phi_{\Delta[\mathrm{HbO}]}$) obtained with the phase synchronization method and with the cross-correlation phasor method. The temporal trend relative to the phasor method in Fig. 2(b) is obtained with a moving window of 20 s. On the contrary, the temporal trend relative to the phase synchronization method plots the instantaneous phase value calculated by the Hilbert transform. The two curves are overall very similar. The discrepancies between them are most probably due to the absence of any averaging procedure in the phase synchronization trend, and they manifest more often when the amplitude of Δ[Hb] is within the noise level or when the phase is close to 360°. Figures 3 and 4 show the histograms of the phase lag distributions obtained with the phase synchronization method (Fig. 3) and cross-correlation method (Fig. 4) during the entire experimental protocol. The distributions are peaked at values close to π radians. The mean phase lags

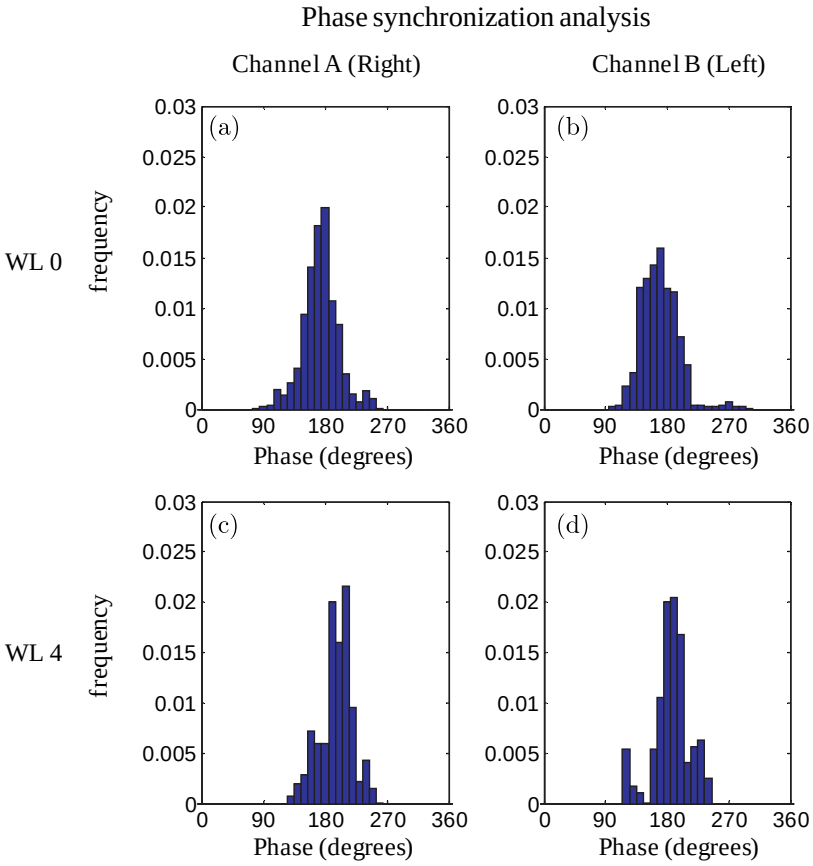

Fig. 3. Histograms of phase distributions obtained with the phase synchronization method on the right side of the forehead (Channel A: panels (a) and (c)) and on the left side of the forehead (Channel B: panels (b) and (d)). The phase distributions measured during workload 0 (WL 0) are in panels (a) and (b), whereas those measured during workload 4 (WL 4) are in panels (c) and (d). The area under the histograms is normalized to 1.

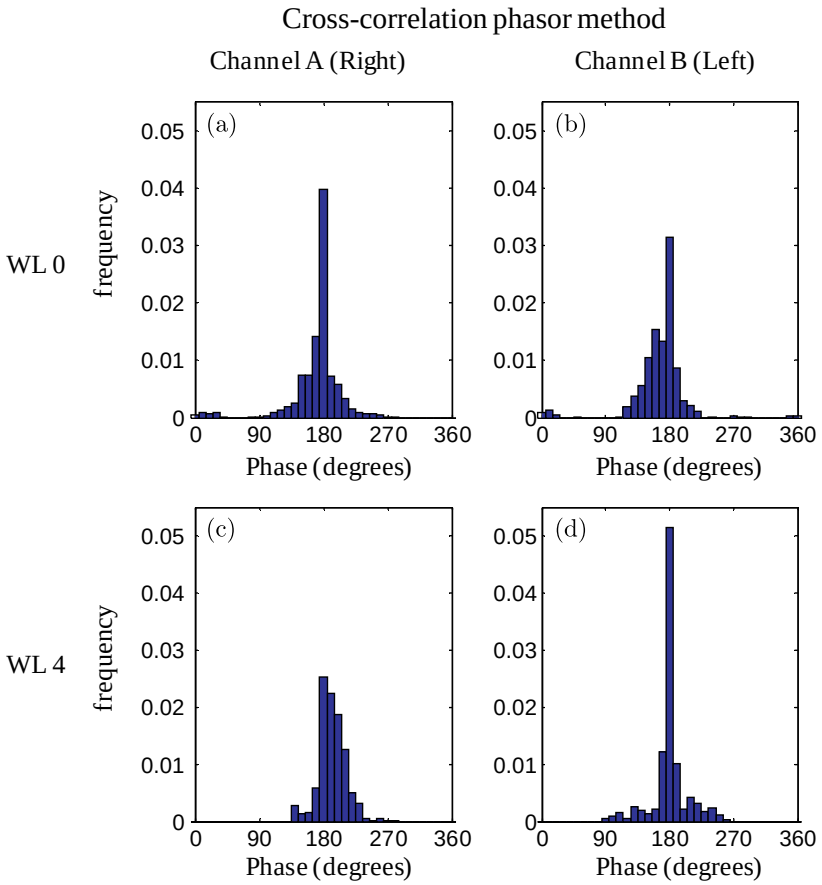

Fig. 4. Histograms of phase distributions obtained with the cross-correlation phasor method on the right side of the forehead (Channel A: panels (a) and (c)) and on the left side of the forehead (Channel B: panels (b) and (d)). The phase distributions measured during workload 0 (WL 0) are in panels (a) and (b), whereas those measured during workload 4 (WL 4) are in panels (c) and (d). The area under the histograms is normalized to 1.

during workloads 0 and 4 are significantly different ($p < 10^{-6}$) according to the Watson−Williams test for the equality of means of two or more distributions.[16] In order to better illustrate this finding, the first two moments (i.e., the average value and the standard deviation) of the phase distributions of Figs. 3 and 4 are used to generate sector diagrams, which are reported in Fig. 5. The average values of the phase lags are indicated by thin vectors for workload 0 and thick vectors for workload 4, whereas the standard deviations of the phase lags are indicated by white sectors for workload 0 and shaded sectors for workload 4. Specifically, the angles of the vectors in Fig. 5, as measured counterclockwise with respect to the horizontal rightward direction, represent the average of the phase lag between [Hb] and [HbO]. The angular widths of the sectors in Fig. 5 represent ± the standard deviation of the [Hb]−[HbO] phase lag distributions around the average. Figures 3−5 show that the phase synchronization method and the cross-correlation phasor method yield comparable results for the distribution of phase lags between LFOs of deoxy- and oxy-hemoglobin concentrations. Therefore, they can be applied interchangeably to describe phase relationship of hemodynamic parameters, at least for linear phenomena.

In our recent work,[12] we have argued that phase lags other than 0° or 180° between oscillations in [Hb] and [HbO] cannot be an artifact due to the limitations of the modified Beer−Lambert law but rather reflect the combination of out-of-phase underlying physiological processes. Such underlying physiological processes, or possibly just the way in which they combine to affect the measured oscillations of [Hb] and [HbO], may be affected by brain activation (caused by the varying components of neural processing induced by the different mental workload in

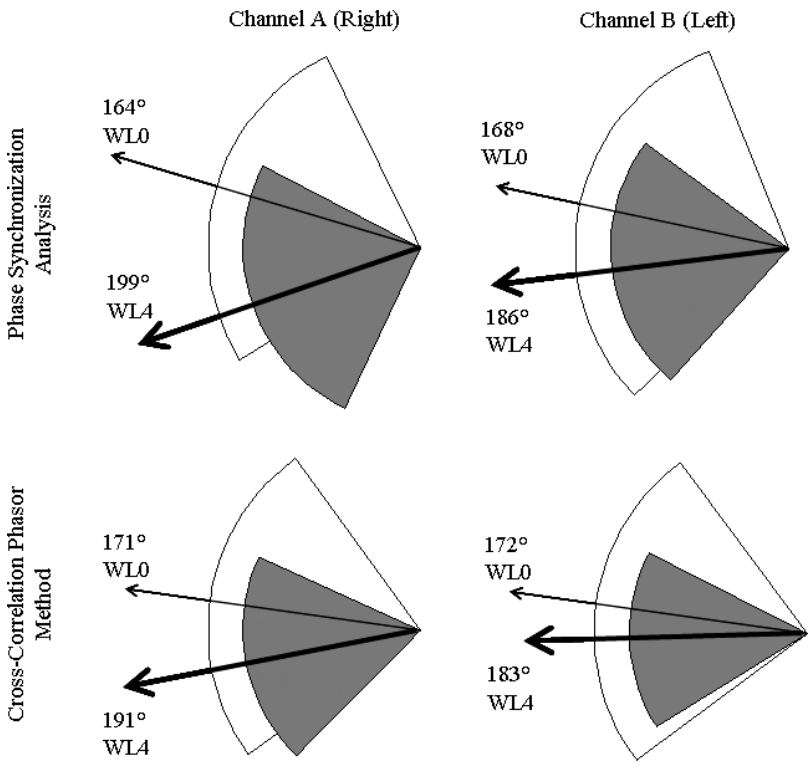

Fig. 5. Vector and sector diagrams of the phase lag between LFOs of [Hb] and [HbO]. Thin vectors and white sectors refer to workload 0 (WL 0), whereas thick vectors and shaded sectors refer to workload 4 (WL 4). Phases in these diagrams are measured counterclockwise from the horizontal rightward direction. The vector directions (and the indicated angular values in degrees) represent average phase lags. The angular width of the sectors represents ± the standard deviation of the phase lag distributions around the average as obtained using circular statistics.

the case of this work) and result in a different relative phase of [Hb] and [HbO] oscillations.

5. Conclusions

In this work, we have reported two methods (one based on phase synchronization analysis, and the other based on cross-correlation phasors) to measure the relative phase of LFOs of cerebral concentrations of [Hb] and [HbO] during two mental tasks involving varying magnitudes of working memory action. Such phase measurements may provide an alternative or complementary approach to more conventional block average procedures to investigate hemodynamic and physiological effects of brain activation. In a pilot experiment on one human subject, we have found a significant difference between the phase lag of [Hb] vs [HbO] LFOs as measured during workload 0 and workload 4. These results are preliminary yet show promise for the use of phase measurements in brain studies. It will be of particular interest to apply this form of analysis to a larger topographic surveillance of the whole cortical surface as well as to larger numbers of subjects. Phase relationships between [Hb] and [HbO] oscillations play an important role not only in the study of cerebral hemodynamic effects of brain activation (as reported here) but potentially also in the spatiotemporal domain of dynamic studies of functional connectivity networks in the brain. The possibility of using this analytical approach, especially in concert with concurrent network correlation techniques derived from electrophysiological measurements, is particularly important. By careful application of cognitive tasks to variably stimulate neural networks, the combination of spatiotemporal phase lags in the vascular connectivity networks and electrophysiological networks should provide a unique and potentially fruitful path for analyzing how neural and metabolic processes integrate in the brain.

Acknowledgment

This research is supported by NIH Grant R01-NS059933 and by NSF Award IIS-0713506.

References

1. M. A. Franceschini, V. Toronov, M. E. Filiaci, E. Gratton, S. Fantini, *Opt. Exp.* **6**, 49 (2000).
2. V. Toronov, A. Webb, J. H. Choi, M. Wolf, L. Safonova, U. Wolf, E. Gratton, *Opt. Exp.* **9**, 417 (2001).
3. H. Obrig, M. Neufang, R. Wenzel, M. Kohl, J. Steinbrink, K. Einhäupl, A. Villringer, *Neuroimage* **12**, 623 (2000).
4. R. P. Kennan, S. G. Horovitz, A. Maki, Y. Yamashita, H. Koizumi, J. C. Gore, *Neuroimage* **16**, 587 (2002).
5. P. Fransson, *Hum. Brain Mapp.* **26**, 15 (2005).
6. M. E. Raichle, A. Z. Snyder, *Neuroimage* **37**, 1083 (2007).
7. M. Reinhard, E. Wehrle-Wieland, D. Grabiak, M. Roth, B. Guschlbauer, J. Timmer, C. Weiller, A. Hetzel, *J. Neurol. Sci.* **250**, 103 (2006).
8. B. R. White, A. Z. Snyder, A. L. Cohen, S. E. Petersen, M. E. Raichle, B. L. Schlaggar, J. P. Culver, *Neuroimage* **47**, 148 (2009).
9. F. A. Kozel, F. Tian, S. Dhamne, P. E. Croarkin, S. M. McClintock, A. Elliott, K. S. Mapes, M. M. Husain, H. Liu, *Neuroimage* **47**, 1177 (2009).
10. H. Zhang, Y. Zhang, C. Lu, S. Ma, Y. Zang, C. Zhu, *Neuroimage* **51**, 1150 (2010).
11. G. Taga, Y. Konishi, A. Maki, T. Tachibana, M. Fujiwara, H. Koizumi, *Neurosci. Lett.* **282**, 101 (2000).
12. F. Zheng, A. Sassaroli, S. Fantini, *JBO Lett.* **15** 040512 (2010).
13. P. Tass, M. G. Rosenblum, J. Weule, J. Kurths, A. Pikovsky, J. Volkmann, A. Schnitzler, H. J. Freund, *Phys. Rev. Lett.* **81**, 3291 (1998).
14. C. Yan, D. Liu, Y. He, Q. Zou, C. Zhu, X. Zuo, X. Long, Y. Zang, *PLoS One* **4**, e5743 (2009).
15. A. Sassaroli, F. Zheng, L. M. Hirshfield, A. Girouard, E. T. Solovey, R. J. K. Jacob, S. Fantini, *JIOHS* **1**, 227 (2008).
16. P. Berens, *J. Statist. Softw.* **31**, 1 (2009).